RSC Advances

ROYAL SOCIETY OF CHEMISTRY

www.rsc.org/advances

A surface-enhanced Raman scattering strategy for detection of peanut allergen-Ara h 1 using bipyramid-shaped gold nanocrystals as substrate with an improved synthesis

Zhou Xiaoyan [a], Li Ruiyi [b], Li Zaijun [a,c]*, Liu Junkang [a], Gu Zhiguo [a] and Wang Guangli [a]

[a:] *School of Chemical and Material Engineering, Jiangnan University, Wuxi 214122, China*

[b:] *The University of Birmingham, Edgbaston,Birmingham, BI5 2TT, United Kingdom*

[c:] *The Key Laboratory of Food Colloids and Biotechnology, Ministry of Education, Wuxi 214122, China*

We reported an improved synthesis of branched gold nanocrystals through the use of sodium dodecylbenzene sulfonate (SDBS) an additive. The introduction of SDBS allows to reduce hexadecyltrimethylammonium bromide to 0.05 M as opposed to 0.1 M in well-established protocols, accelerates the growth rate of gold seeds and improves the side growth over the twin boundaries that results in the formation of five elongated branches with the highest point of each branch bisecting the branch into two halves. The obtained bipyramid-shaped gold nanocrystal has been applied to surface-enhanced Raman scattering detection of peanut allergen-Ara h 1 in food samples with the detection limit of 3.3×10^{-15} M (N/S=3).

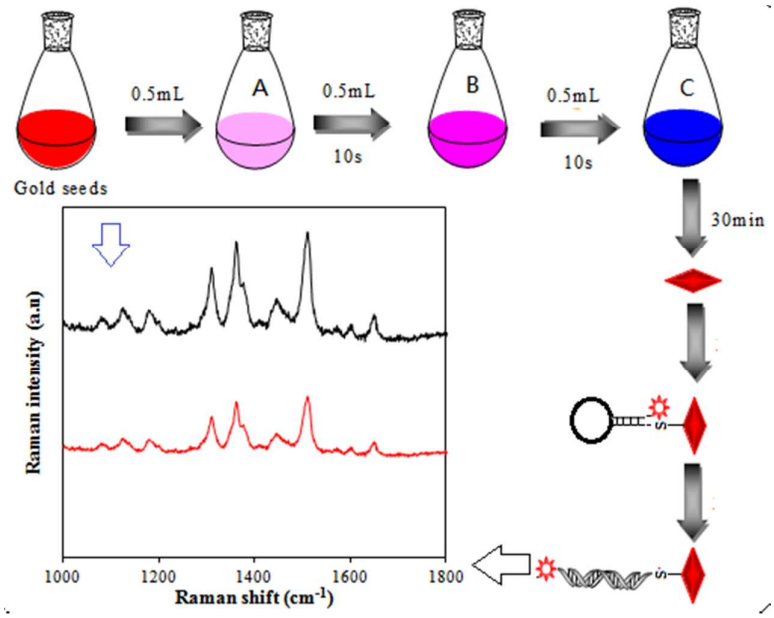

Cite this: DOI: 10.1039/c0xx00000x

www.rsc.org/xxxxxx

ARTICLE TYPE

A surface-enhanced Raman scattering strategy for detection of peanut allergen Ara h 1 using bipyramid-shaped gold nanocrystals substrate with an improved synthesis

Zhou Xiaoyan,[a] Li Ruiyi,[b] Li Zaijun,[a,c]* Liu Junkang,[a] Gu Zhiguo[a] and Wang Guangli[a]

Received (in XXX, XXX) Xth XXXXXXXXX 20XX, Accepted Xth XXXXXXXXX 20XX
DOI: 10.1039/b000000x

Branched and star-shaped gold nanocrystals have received significant attention owing to unique optical and electronic properties, but the most of gold nanocrystals have zero-dimensional shape with varying numbers of branches coming from a quasi-spherical core. Here, we reported an improved mthod for synthesis of branched gold nanocrystals through use of sodium dodecylbenzene sulfonate (SDBS) additive. The introduction of SDBS allows to reduce hexadecyltrimethylammonium bromide to 0.05 M, accelerate the growth rate of gold seeds and improve the side growth over twin boundaries. This leads to form five elongated branches with the highest point of each branch bisecting branch into two halves. The resulting bipyramid-shaped gold nanocrystals (BPGNs) offer an excellent monodispersion and thus morphology separation process for BPGNs is not necessary before use. The hybridization of target DNA with probe DNA will result in sensitive SERS response. The SERS intensity linearly decreases with the increase of target DNA concentration in the range from 10^{-14} to 10^{-8} M. The detection limit was 3.3×10^{-15} M (N/S=3). The analytical method provides significant advantage of sensitivity, selectivity and repeatability compared with other SERS methods using gold nanoparticles, gold nanorods and star-shaped gold nanocrystals, it has been successfully applied to detect peanut allergen Ara h 1 in food samples.

1 Introduction

Nanoscale materials possess unique optical,[1] catalytic,[2] magnetism[3] and sensing[4] properties. These properties seriously depend the sizes and shapes of bulk materials.[5-7] Their physicochemical behaviours can be altered by controlling their sizes and shapes.[8-10] Among noble metal nanomaterials, gold nanocrystals are one of the most stable noble metal materials and have widespread application prospect in physical chemistry, electronics, biology, and many other fields.[8,11] Recently, the gold nanocrystals with sharp edges and tips have attracted much attention owing to its special structures and unique localized surface plasmon resonance. To date, these gold nanocrystals have been applied as ideal substrate for the surface enhanced Raman scattering (SERS) detection.[12-15]

The most accepted approach for generation of gold nanocrystals is the seed-mediated synthesis. The method includes surfactant-directed growth of nanomaterials from gold seeds. The seeds were prepared by reduction of chlorauric acid with strong reducing agent. The growth step involves addition of the seed solution to the growth solution with more chlorauric acid and weak reducing agent in presence of cationic surfactant. A cationic surfactant, hexadecyltrimethylammonium bromide (CTAB), was often acted as a soft template in the growth solution and structure-directing agent to direct the formation of gold nanocrystals.[16,17] Although CTAB do good for controlling shapes of gold nanocrystals, it restrain further application of gold nanocrystals. On the one hand, the gold nanocrystals prepared by CTAB have been reported to be cytotoxic.[18,19] The side effect may emerge due to incomplete purification of gold nanocrystals or desorption from the bound bilayer when contacting with biological molecules. On the other hand, these capped agents adhere tightly on the surface of gold nanocrystals, which are difficult to be removed from the surface. This will limit some applications in the SERS which strongly depends on surface of nanoparticals.[20,21] The development of no-surfactants or decrease surfactant is of great significance.

The peanut and its food derivatives belong to the “big eigh” group of foods that account for the majority of food allergies, along with milk, eggs, fish, crustaceans, wheat, tree nuts, and soybean products. Peanut allergy has a worldwide prevalence of 0.5-2%, which the prevalence appears to be increasing.[22,23] The symptoms of peanut allergy range from mild oral allergy syndrome to anaphylactic reactions, and even death. There is no cure for the peanut allergy. Therapy focuses on primarily peanut avoidance, early recognition of symptoms brought on by the accidental ingestion, and pharmacologic treatment of adverse reactions.[24-27] The names for allergens Ara h 1–11 are officially recognized by Allergen

Nomenclature Sub-Committee of International Union of Immunological Societies. Ara h 1 is a major peanut allergen, thus its detection is important. The methods for detecting DNA to reflect the existence of allergens such as PCR[16] and real-time PCR[17] have been developed. Recently, many modern technologies have also been reported for detection of Ara h 1, including electrochemical sensor,[18] liquid chromatography mass spectrometry,[19] gas chromatography mass spectrometry[20] and flow cytometric method,[28] These methods offer good detection limits, but they are time-consuming and often need use of expensive reagents or instruments. The development of a rapid and convenient method for food allergen analysis is extremely desirable.

The study focuses an improved synthesis of branched gold nanocrystals through use of sodium dodecylbenzene sulfonate (SDBS) anionic surfactant as additive. The result demonstrated that the introduction of SDBS allows to reduce CTAB concentration to 0.05 M, accelerate the growth rate of gold seeds and improve the side growth over the twin boundaries that results in the formation of five elongated branches with the highest point of each branch bisecting the branch into two halves. The resulting bipyramid-shaped gold nanocrystals (BPGNs) were used as the substrate for SERS detection of peanut allergen-Ara h 1. The analytical method presents significant advantage of sensitivity, selectivity and repeatability compared with other SERS methods using gold nanoparticles, gold nanorods and star-shaped gold nanocrystals.

2 Experimental

2.1 Materials and reagents

Chlorauric acid ($HAuCl_4$) and (3-aminopropyl)-triethoxysilane (APTES) were purchased from Sigma-Aldrich Chemical Company (Mainland, China). Sodium borohydride, SDBS, hydrochloric acid, silver nitrate, trisodium citrate dihydrate, L-ascorbic acid and CTAB were purchased from Shanghai Chemical Company (Shanghai, China) and used without further purification. All synthetic oligonucleotides were purchased from Sangon Biotech Co., Ltd. (Shanghai, China). The sequences of oligonucleotides used in this work were listed in the following. Oligonucleotides 1 (stem-loop probe): 5'-HS-C6-GCG AGG TTC CGT GGC TGC TGA TGA CTT GGT CCT CGC-biotin-3', oligonucleotides 2 (complementary target): 5'-ACC AAG TCA TCA GCA GCC ACG GAA-3', oligonucleotides 3 (single mismatch): 5'-ACC AAG TAA TCA GCA GCC ACG GAA-3', and oligonucleotides 4 (non-complementary): 5'-GTT CGA CTG CTG ATG ATT GTA AGG-3'.The loop sequence of the probe is the conserved sequence of Ara h 1-the main allergen of peanut. Ultrapure water (18.2 MΩ cm) purified from a Milli-Q purification system was used throughout the experiment.

2.2 Apparatus

Surface plasmon resonance absorption spectra were recorded by a TU-1901 spectrometer in absorbance mode with a DH-2000 deuterium and tungsten halogen light source (Beijing Purkinje General Instrument Co., Ltd., China). Scanning electron microscope (SEM) analysises were carried out in a HITACHI S4800 field emission scanning electron microscope. SEM sample was prepared by placing a drop of gold nanocrystals onto sillicon wafer. The solvent was evaporated under an infrared lamp. Raman spectrum was obtained by HITACHI S4800 field emission scanning electron microscope. Raman spectra were recorded by a HR800 Raman microprobe with a 785 nm laser excitation.

2.3 Synthesis of gold nanocrystals

The citrate-stabilized gold seeds were prepared via the procedure as reported previously.[1] Typically, a 0.1 mL of 0.025 M trisodium citrate solution was mixed with 9.9 mL of 0.25 mM $HAuCl_4$ solution. Then, a 0.3 mL freshly prepared ice-cold 0.01 M $NaBH_4$ in 0.025 M trisodium citrate solution was injected into the mixted solution under vigorous stirring (500 rpm). The solution changed from colorless to orange-red immediately, indicating the formation of gold seeds. After 2 min, the stirring was stopped. The resulting seed solution was kept for at least 2 h before use.

An imporved multi-step growth method was used to prepare BPGNs.[29] In a typical procedure, three 20 mL of vials labeled A, B or C were used. A growth solution of sufficient volume was prepared containing 0.25 mM $HAuCl_4$, 0.05 M CTAB, 0.25 mM SDBS and 0.25 mM HCl. To each of these vials was added 4.5 mL of growth solution. Next, 0.05 mL of 0.01 M $AgNO_3$ solution was introduced into only one vessel labled solution C. After gentle mixing of the solution, 25 μL 0.08 M ascorbic acid was added to every vial and the solution color turned colorless, indicating the reduction of Au^{3+} to Au^{+} species. Next, 0.5 mL of the seed solution was rapidly injected into vial A. After being vigorously stirred for 10 s, 0.5 mL solution in vial A was withdrawn and injected into vial B. Similarly, 0.5 mL of solution in vial B was withdrawn and injected into vial C after being stirred for 10 s. The colorless solution in vial C slowly turned violet blue. After reaction under the temperature of 30□ for 1 h, the solution was centrifuged to remove CTAB from the solution and redispersed into ultra pure water.

2.4 Extraction of the peanut DNA from food samples

The amount of food sample was crushed using the tissue triturator and then dispersed in 50 mL of the PBS by ultrasonication. Then, it was centrifugated for 10 min at 3000 r/min and 4□. After discarding the supernatant, lipids on the tube wall were rubbed out by absorbent cotton. Then, a 10 mL of PBS buffer was added to dissolve sediment. Repeat above steps for three times. After discarding the supernatant and rubbing out lipids, an extraction buffer (0.2 M Tris/HCl pH 7.5, 0.25 M NaCl, 25 mM EDTA, 0.5%SDS) was added to dissolve the pellet, followed by 20-min incubation at 65□. Then, 250 μL of cold phenol/chloroform/isoamyl alcohol (25:24:1) were added. After centrifugation for 10 min at 12000 r/min and

4□, a 400 μL of pre-cooling isopropyl alcohol were added to the supernatant, followed by a 20-min incubation at -20□. After centrifugation for 10 min at 12000 r/min, 4□, 250 μL of ethanol were added to wash the pellet. The supernatant was then discarded and the pellet was re-suspended by adding 50 μL of micro-filtered water. At last, the concentration of the extracted DNA was determined by UV measurement.

2.5 Preparation of SERE substrate

The SERS substrates were fabricated by depositing BPGNs onto the surface of silicon wafer through self-assembly. In a typical procedure, silicon wafer was cleaned by immersion in a mixture containing 30% H_2O_2 and concentrated H_2SO_4 with a volume ration of 3:7 heat to 80□ for 2 h. After cooling down to room temperature, the silicon wafer was washed with ultrapure water and then dried under nitrogen. Then, the silicon wafer was immersed in a APTES ethanol solution with the volume ration of 1% for 12 h at room temperature, followed by being rinsed in eathanol with sonication 3 times and dried with nitrogen. After centrifugation, a 1.0 mL of 5.0 mM PVP was added in 5 mL of BPGNs solution under vigorous stirring for 30 min. Then, the above silicon wafers were soaked into the mixture for 48 h. The gold films used as SERS substrates formed after the BPGNs self-assmbling uniformly onto the surface of the silicon.

2.6 The SERS detection of DNA

The typical detection of target DNA by the SERS was described as follows: first, 10 μL of 0.2 μM probe DNA was added to the Au substrate and kept at 4□ overnight, followed by rinsing with PBS thoroughly to remove nonbonding probe DNA and drying with a gentle flow of nitrogen. Then, 5 μL of the target DNA was deposited on the each functionalized substrate surface and kept at 37□ for 30 min. After the hybridization, the resultant substrate was washed by the PBS to remove non-hybridized target DNA and dried with nitrogen before SERS detection.

3 Results and discussion

3.1 Synthesis of bipyramid-shaped gold nanocrystals

The seeded growth of gold nanocrystals in aqueous medium has been well-documented in terms of control over gold nanocrystals size and shape uniformity. The original idea was to use micelles formed by CTAB as soft template to direct the formation of gold nanocrystals. To improve optical properties and biocompatibilities, two anionic surfactants were used as additives to cooperate with CTAB for synthesis of BPGNs in the study. **Fig.1** shows surface plasmon resonance absorption spectra of the gold nanocrystals prepared by using the improved method in absence of additives and in presence of sodium dodecyl sulfate (SDS) and SDBS. It can be seen that three kinds of gold nanocrystals are of very similar peak shapes that give rise to a transverse plasmon resonance absorption centered at about 600 nm and a long tail into near-infrared region. However, the intensity of these absorption peaks exists quite difference. The intensity of the absorption peaks using the additive is much higher than that of the gold nanocrystals made in absence of additives as well as the reported method. The intensity of absorption spectrum reaches the maximum when SDBS was employed for the synthesis. Moreover, the result also demonstrates that SDBS can promote the formation of BPGNs and the concentration of CTAB in the growth solution can be reduced to 0.05 M. This not only reduces the material cost and purification step, but also does good to make widely use of BPGNs with low biotoxicity in some special fields such as bio-labeling and biological detection.

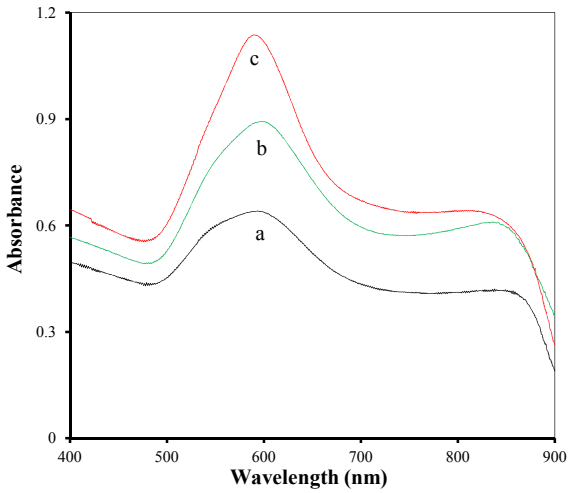

Fig. 1 Surface plasmon resonance absorption spectra of gold nanocrystals made using the improved method in absence of additives (a) and presence of SDS (b) and SDBS (c)

SEM images of the gold nanocrystals made by the improved method in absence of additives, and presence of SDS and SDBS and the reported method were shown in **Fig.2**. By the improved method in absence of additives, the final products were not fully grown with few particularly shap edges as well as inadequately tips. The gold nanocrystals obtained by the improved method in presence of SDS exist many shape impurities, inculding star-shaped and agglomerate nanoparticles. However, the uniform and hyper-branched BPGNs with plenty of tips and sharp edges were obtained in presence of SDBS. The side growth over twin boundaries results in the formation of five elongated branches with the highest point of each branch bisecting the branch into two halves. When SDBS was absent with the CTAB of 0.1 M, the morphology became random-shaped. Since the stability and reproucibility of gold nanocrystals served as SERS substrates strongly depend on their morphologies, it is an urgent need to prepare gold nanocrystals with high quality and mondisperse morphology. Thus, the BPGNs obtained by the improved method can be directly applied to the SERS detection with no need of further shape separation. Moreover, we also investigated the effect of the standing time on spectrum of the BPGNs solution. The result shows that the spectrum of BPGNs has almost no change within 10 weeks at ambient temperature, indicating that BPGNs

made in the SDBS system is optically stable. This is very beneficial to improve the reproducibility and precision in the analysis application.

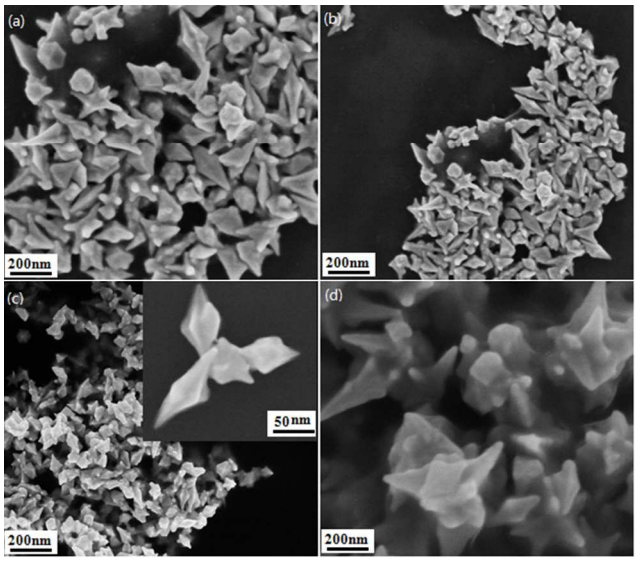

Fig.2 SEM images of gold nanocrystals made using the improved method in absence of additives (a) and presence of SDS (b), SDBS (c) and the reported method (d)

The formation process of BPGNs was systematically investigated by measuring surface plasmon resonance absorption spectra of gold nanocrystals made at various time points during the growth of the gold nanocrystals. **Fig.3**A gives the absorption spectra of BPGNs taken from 0 min to 120 min. It can be observed that the surface plasmon absorption intensity of gold nanocrystals increases progressively, indicating continuous formation of BPGNs. Within the first hour of the reaction, the absorption spectrum consists of a transverse absorption band at approximately 600 nm and a longitudinal absorption tail into near-infrared region. The transverse absorption band exceeds the maximum after 1 h of the reaction, indicating that the growth of nanocrystals nearly completed. Further, the reaction rate of gold nanocrystals made by the improved method and the reported method was shown in Fig.3B. It reveals that the reaction rate of the improved method using SDBS as the additive is obviously faster than the traditional approach. The faster growth rate of BPGNs should be attributed to the reduction of Br^- concentration, because certain amount of Br^- absorbing on the surface of gold nanocrystals controls the growth rate on the different facet. Once there are too many Br^- on the surface of gold nanocrystals, the growth rate of gold nanocrystals will be restricted. In contrast, the introduction of SDBS with a lower CTAB concentration will result in a shorter time for the growth of BPGNs.

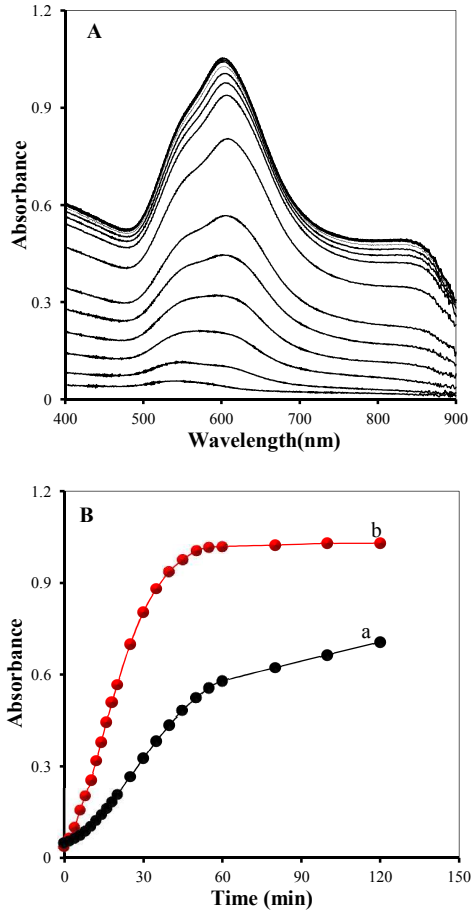

Fig.3A: Surface plasmon resonance absorption spectra of gold nanocrystals made using the improved method when the seed growth time change from 0 min to 120 min (from inside to outside). B: Relationships of the absorbance at 600 nm of gold nanocrystals made by the improved method (b) and the reported method (a) with growth time

The morphology transformation of BPGN intermediate products at different reaction time was shown in **Fig.4**. These representative SEM images illustrate the evolution of BPGN from gold seed to fully-grown one. Fig.4a manifests a preliminary formed bipyramid-shaped gold nanopartical with a size of about 90 nm and some rounded tips at just 5 min after the reaction. It is not obvious that tiny protrusions appear near middle section. After 10 min of the reaction, the average height of particle size increases rapidly to 130 nm, and it shows an appearance of the pentagonal bipyramind. A 20 min later, the branched nanocrystal shows a more substantial increase in their sizes to 200 nm and a discernible twin boundaries along the long axe. At the time point of 30 min, the side branches became clearly distinguished. The side branches have become developed slowly during the whole process. The images of BPGNs obtained at 1 h and 12 h maintained exactly the same, so the fully grown BPGN was obtained for 1 h with a length of 200 nm and a base width of 80 nm.

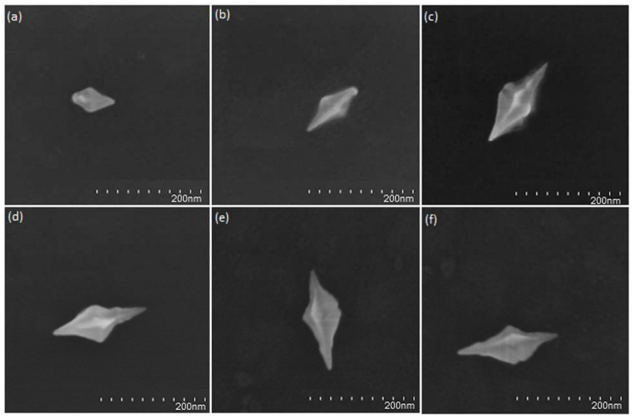

Fig.4 SEM images of the intermediates by investigating the BPGNs formed after reaction for 5, 10, 20, 30, 60 min and 10 h

SDBS and SDS have similar molecular structure and the only distinction is that the former has a rigid benzene ring. Thus, we think that the special structure of SDBS plays an important role in the formation of BPGNs. To understand the action principle of SDBS, a possible micelle structure formed on the surface of gold nanocrystal was suggested in **Fig.5**. Here, CTAB bilayer consists of two surfactant leaflets. One is associated with the gold surface via the quaternary ammonium head groups, and the other has the surfactant head groups facing the aqueous media. This bilayer assembly is energetically favoured as it guarantees hydrophobic interactions between the surfactant tails in the bilayer core and hydrophilic interactions of the charged head group with the aqueous media at the nanoparticle-solvent interface. Three distinctive interfaces can be described for the system, the BPGNs-CTAB interface, the CTAB bilayer itself, and the outer CTAB exposed to the bulk solution.[30,31] When negative charged SDBS was introduced, CTAB will coordinate with SDBS to form stable micelle structure by electrostatic interaction and hydrophobic function. The hydrophobic benzene ring of SDBS tends to penetrate into the hydrophobic alkyl chain of the CTAB monomer. Meanwhile, its sulfonic acid groups stands perpendicular to the surfactant and projects radially from the surface of the micelle into the bulk aqueous solution. The above two factors change synergistically the micellar packing parameter p=v/Al, where v is the effective volume of the hydrophobic chain, A is the effective area of the polar headgroup, and l is the length of the hydrocarbon chain.[28] Insertion of the phenyl moiety of the salts increases the v of the CTAB micelle. Anion association reduces the micellar surface charge and decreases A by reducing the electrostatic repulsion between the quaternary ammonium groups, promoting the spherical to rodlike micellar transition. As a result, the repulsive force of hydrophilic groups decreases greatly and the long hydrophobic chains of CTAB can be more easily to arrange neatly on the surface of the nanoparticles. All these improve the stability of micelles formed by CTAB and its surface activity. This can result in the reduce of CTAB and an improved BPGNs with the monodisperse morphology.

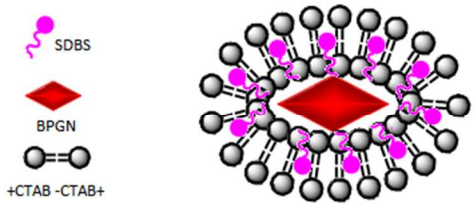

Fig.5 Possible micelle structure formed on the surface of BPGN

3.2 SERS behavior of different gold nanocrystals

Gold nanocrystals can sustain surface plasmon resonance in presence of various organic molecules and make them suitable for plasmonic application and optical enhancement such as SERS detection.[32,33] The branched gold nanocrystals should be more suitable for the SERS detection because of sharp edges, tips and high surface areas. To evaluate the SERS behavior of various gold nanocrystals, Rhodamine 6G was empolyed as the SERS probe to explore SERS application of gold nanospheres, gold nanorods, star-shaped gold nanocrystals and BPGN substrate. **Fig.6** clearly displays that the BPGN substrate offers the highest SERS signal, while the nanosphere substrate exhibits the lowest SERS response. It is reported that Rhodamine 6G is chemisorbed on the surface of gold nanocrystals via ethylamino group when Rhodamine 6G mixed with gold nanocrystals. The gaps between adjacent gold nanocrystals have been known to offer extremely intense local electromagnetic field upon optical excitation, which could lead to large SERS enhancement for the active molecular vibration mode. Compared with other gold nanocrystals, BPGN offers an increased surface roughness as well as the presence of sharp edges and tips, which lead to more "hot spots" and more sensitive SERS response.

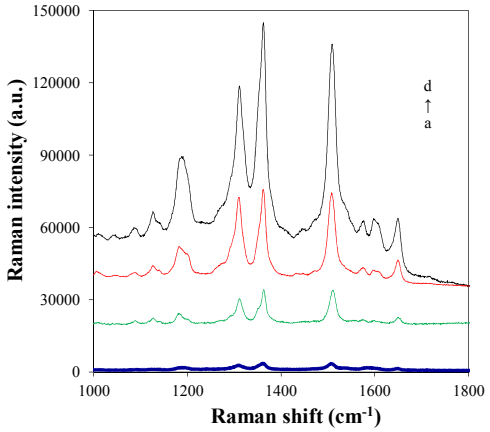

Fig.6 Surface-enhanced Raman spectra of Rhodamine 6G (1.0×10^{-5} M) on gold nanospheres (a), gold nanorods (b), star-shaped gold nanocrystals (c) and BPGN (d) substrates

3.3 Sensor operation principle

SERS enhancement is often attributed to the electromagnetic and chemical enhancement.[34] The former

is based on the amplified local electromagnetic field owing to optical excitation of surface plasmon resonances of the nanoscale metals with a coarse surface. The latter mainly results from a short-range e□ect of charge transfer between adsorbate and metal surface when they are close enough to each other. It is widely accepted that the combination of the electromagnetic and chemical enhancements cause the SERS enhancement. In the work, BPGN was investigated as the substrate for SERS detection of peanut allergen-Ara h 1. Here, a probe DNA was thiol-modified at its 5' end, and also Cy3-labeled at its 3' end. The Cy3-tagged "molecular beacon"-like probe DNA was firmly attached to the surface of BPGN to form a stem-loop structure by self-assembling via gold-thiol bonding. The actual hybrid sequence is situated in the loop part of the single strand, and the stem is formed by base paring the two complementary arm sequences at either side of the loop. If the target DNA is absent, the stem-loop probe is "closed" and the Cy3 unit is located very close to the gold surface. On the hybridization of target DNA the conformation will undergo a thermodynamically driven change to an "open" structure, forming a thermodynamically stable and rigid double-stranded DNA helix. As a result, the Cy3 at the 3'-end will be displaced from the surface of the BPGN and results in an obvious decrease of the SERS signal. Therefore, we can get the conclusion that the SERS enhancement will rapidly decrease with the increase of the distance between the adsorption molecule and the BPGN surface.

3.4 Analytical characteristics

Further investigation of the possibility for quantitative target DNA detection was carried out by hybridizing it with various concentrations of the target DNA, and then the SERS response of as-prepared substrate was measured. **Fig.7A** shows that the SERS intensity of Cy3-tagged DNA is gradually decreased with the increase of complementary target DNA concentration. This is because higher complementary target DNA concentration opens more stem-loop probe structures, that lead to obvious decrease of the SERS signal. The relationship of SERS response with the target DNA concentration was shown in Fig.7B. With the increase of target DNA concentration the Raman intensity decreases linearly in the range from 10^{-14} M to 10^{-8} M. The linear equation was I=-1211C-5974, with a statistically significant correlation coefficient of 0.9991. Detection limit of the proposed method was 3.3×10^{-15} M that was obtained from the signal-to-noise characteristics of these data (S/N=3). The SERS substrate is measured at several different positions to demonstrate the reproducibility of this SERS assay. The results are almost the same in the intensity as well as shape of peaks, which demonstrates the high reproducibility of the prepared SERS substrate. In addition, we tested the reproducibility for a number of gold substrate. The SERS spectra were taken from five structures and the intensities of 1512.38 cm^{-1} band show good reproducibility only with slight intensity fluctuations. This result demonstrates the reliable reproducibility of gold substrate. The stability of the DNA substrate is evaluated on a 15-day period. When it is stored in the refrigerator at 4□, the SERS signal of it retained 99.6% of its initial response. This indicated that the developed DNA SERS substrate had a good stability. These analytical parameters are better than that of the reported methods for the detection of peanut allergen-Ara h 1.[30-33]

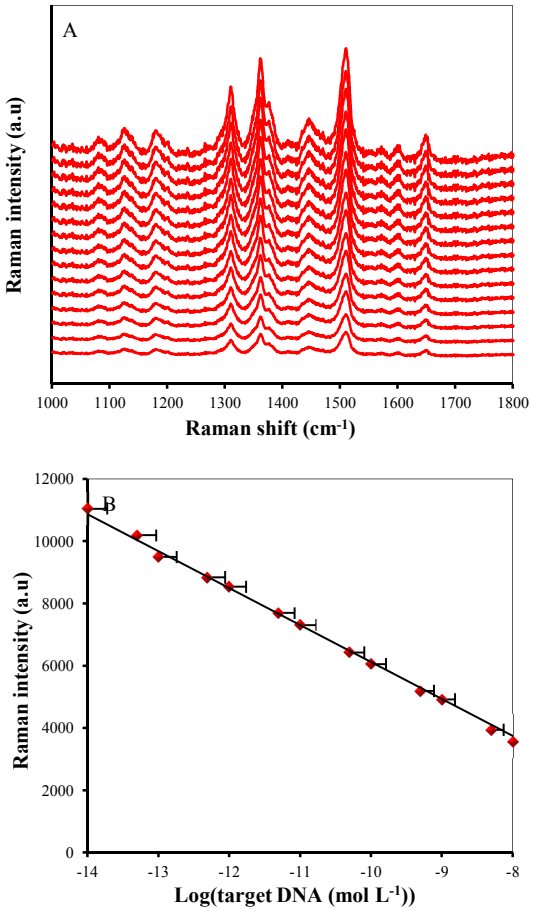

Fig.7A: SERSs of probe DNA hybridized with different concentration of target DNA (from top to bottom are 1×10^{-14}, 5×10^{-14}, 1×10^{-13}, 5×10^{-13}, 1×10^{-12}, 5×10^{-12}, 1×10^{-11}, 5×10^{-11}, 1×10^{-10}, 5×10^{-10}, 1×10^{-9}, 5×10^{-9}, 1×10^{-8}, 5×10^{-8} and 1×10^{-7} M, respectively). B: The relationship between Raman intensity at 1512.38 cm^{-1} and log (target DNA (M)).

To verify the high selectivity of the as-prepared DNA SERS sensor, SERS signals were obtained by adding equal amount of various DNA sequences (complementary DNA, single mismatch DNA and non-complementary DNA). **Fig.8** indicates that the SERS intensity is significantly reduced in the presence of complementary target DNA, while strong SERS signal from Cy3-labeled DNA were observed when the single mismatch DNA was added. This is probably because the intensity of the Raman signals increase with the decrease of the distance between adsorption molecules and the surface of the substrate. So, the most obvious enhancement is available when the reporter DNA in the “closed” state. All these indicate the stem-loop DNA sensor offers a high specificity and has a great advantage in mismatched discrimination.

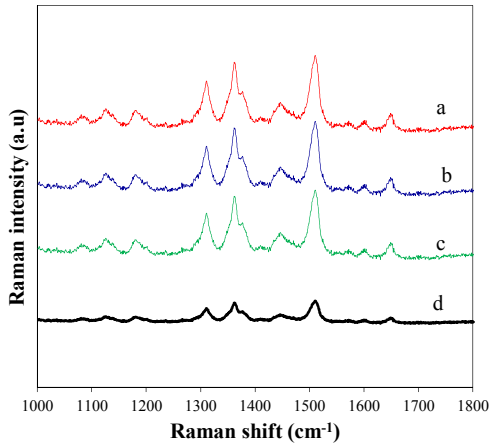

Fig.8 SERS patterns of Cy3 labeled probe DNA (a) and hybridized with non-complementary DNA (b), one base mismatch DNA (c) and complementary DNA (d)

3.5 Sample analysis

The feasibility of the newly developed method for possible applications was investigated by analyzing food samples. All food samples were purchased from Wuxi city. The spike and recovery experiments were performed by measuring the SERS responses to the sample in which the known concentrations of peanut allergen-Ara h 1 were added. The concentration of peanut allergen-Ara h 1 in food sample was determined from the calibration curve and the value was used to calculate the concentration in the original sample. The mean±SD of each sample and recovery of each spiked sample were calculated, and the values are reported in **Table 1**. The recovery of peanut allergen-Ara h 1 for spiked samples analysis is in the range 96.1-105.7 %. These indicated proposed method has a good accuracy and precision.

Table 1 Determination of peanut allergen-Ara h 1 in food samples (n=6)

Samples	Peanut allergen-Ara h 1 found by proposed method (pM)	Peanut allergen-Ara h 1 found by LC-MS (pM)
Peanut butter	1.21±0.15	1.25±0.12
Spiced peanuts	4.11±0.19	4.08±0.22
Peanut brittle	0.21±0.05	0.23±0.03
Fishskin peanuts	7.01±0.32	6.87±0.52
Egg crisp peanut	0.91±0.09	0.92±0.06

3.6 Conclusions

The study demonstrated an improved synthesis of BPGNs through the use of SDBS. The use of SDBS reduces the concentration of CTAB to 0.05 M, accelerate the growth rate of gold seeds and improve the side growth over the twin boundaries. Because the increased surface roughness and sharp edges or tips that lead to more "hot spots" and much higher SERS activity, the as-prepared monodisperse BPGNs were empolyed as a novel SERS substrate for the detection of DNA hydrization with a higher sensitivity. The method provides significant advantage of sensitivity when compared with using gold nanoparticles, gold nanorods and star-shaped gold nanocrystals, and can be widely used in food safety, environmental monitoring and bioanalysis.

Acknowledgements

The authors acknowledge the financial support from the National Natural Science Foundation of China (No.21176101), the Fundamental Research Funds for the Central Universities (No.JUSRP51314B), MOE & SAFEA for the 111 Project (B13025) and the country "12th Five-Year Plan" to support science and technology project (No. 2012BAK08B01).

Notes and references

[a] *School of Chemical and Material Engineering, Jiangnan University, wuxi, China. Fax:86051085811863; Tel:13912371144; e-mail: zaijunli@263.net*
[b] *The University of Birmingham, Edgbaston, Birmingham, BI5 2TT, United Kingdom*
[c] *The Key Laboratory of Food Colloids and Biotechnology, Ministry of Education, Wuxi 214122, China*

1 T. Kim, D.S. Kim, B. Y. Lee, Z. H. Kim and S. Hong, *Advanced Materials*, 2009, **21**, 1238.
2 M. A. El-Sayed, *Accounts of Chemical Research*, 2001, **34**, 257.
3 V. F. Puntes, K. M. Krishnan and A. P. Alivisatos, *Science*, 2001, **291**, 2115.
4 C. A. Mirkin, R. L. Letsinger, R. C. Mucic and J. J. Storhoff, *Nature*, 1996, **382**, 607.
5 R. Sardar, A. M. Funston, P. Mulvaney and R. W. Murray, *Langmuir*, 2009, **25**, 13840.
6 M. E. Stewart, C. R. Anderton, L. B. Thompson, J. Maria, S. K. Gray, J. A. Rogers and R. G. Nuzzo, *Chemical Reviews*, 2008, **108**, 494.
7 J. Han, Y. Liu and R. Guo, *Journal of the American Chemical Society*, 2009, **131**, 2060
8 A. R. Tao, S. Habas and P. Yang, *Small*, 2008, **4**, 310.
9 Y. Xia, Y. Xiong, B. Lim and S. E. Skrabalak, *Angewandte Chemie-International Edition*, 2009, **48**, 60.
10 P. C. Ray, *Chemical Reviews*, 2010, **110**, 5332.
11 C. Burda, X. B. Chen, R. Narayanan and M. A. El-Sayed, *Chemical Reviews*, 2005, **105**, 1025.
12 L. Rodriguez-Lorenzo, R. A. Alvarez-Puebla, F. Javier Garcia de Abajo and L. M. Liz-Marzan, *Journal of Physical Chemistry C*, 2010, **114**, 7336.
13 Q. Su, X. Ma, J. Dong, C. Jiang and W. Qian, *Acs Applied Materials & Interfaces*, 2011, **3**, 1873.
14 C. Hrelescu, T. K. Sau, A. L. Rogach, F. Jackel and J. Feldmann, *Applied Physics Letters*, 2009, **94**, 153113-1.
15 E. N. Esenturk and A. R. H. Walker, *Journal of Raman Spectroscopy*, 2009, **40**, 86.
16 G. Wei, L. Wang, Z. G. Liu, Y. H. Song, L. L. Sun, T. Yang and Z. A. Li, *Journal of Physical Chemistry B*, 2005, **109**, 23941.
17 A. M. Alkilany, R. L. Frey, J. L. Ferry and C. J. Murphy, *Langmuir*, 2008, **24**, 10235.
18 T. Niidome, M. Yamagata, Y. Okamoto, Y. Akiyama, H. Takahashi, T. Kawano, Y. Katayama and Y. Niidome, *Journal of Controlled Release*, 2006, **114**, 343.
19 C. J. Murphy, A. M. Gole, J. W. Stone, P. N. Sisco, A. M. Alkilany, E. C. Goldsmith and S. C. Baxter, *Accounts of Chemical Research*, 2008, **41**, 1721.
20 D. Graham, *Angewandte Chemie-International Edition*, 2010, **49**, 9325.
21 R. A. Halvorson and P. J. Vikesland, *Environmental Science & Technology*, 2010, **44**, 7749.
22 C. Bindslev-Jensen, D. Briggs, M. Osterballe, *Allergy*, 2002, **57**, 741.
23 M. Osterballe, T.K. Hansen, C.G. Mortz, A. Host, C. Bindslev-Jensen, *Pediatr. Allergy Immunol.*, 2005, **16**, 567.
24 S.A. Bock, A. Munoz-Furlong, H.A.Sampson, *J. Allergy Clin. Immunol.*, 2001, **107**, 191.

25 G. Roberts, *Pediatr. Allergy Immunol.*, 2007, **18**, 543.
26 H.S. Skolnick, M.K. Conover-Walker, C.B. Koerner, H.A. Sampson, W. Burks, R.A. Wood, *J. Allergy Clin. Immunol.*, 2001, **107**, 367.
27 Mari, E. Scala, P. Palazzo, S. Ridolfi, D. Zennaro, G. Carabella, *Cell Immunol.*, 2006, **244**, 97.
28 S. R. Nicewarner-Pena, R. G. Freeman, B. D. Reiss, L. He, D. J. Pena, I. D. Walton, R. Cromer, C. D. Keating and M. J. Natan, *Science*, 2001, **294**, 137.
29 H.L. Wu, C.H. Chen, and M.H. Huang, *Chem. Mater.*, 2009, **21**, 110.
30 C.J. Murphy, L.B. Thompson, A.M. Alkilany, P.N. Sisco, S.P. Boulos, S.T. Sivapalan, J.A. Yang, D.J. Chernak, and J.Y. Huang, *J. Phys. Chem. Lett.*, 2010, **1**, 2867.
31 C.J. Murphy, L.B. Thompson, D.J. Chernak, J. A. Yang, S.T. Sivapalan, S.P. Boulos, J.Y. Huang, A.M. Alkilany and P.N. Sisco, *Current Opinion in Colloid & Interface Science*, 2011, **16**, 128.
32 R. Baigorri, J. M. Garcia-Mina, R. F. Aroca and R. A. Alvarez-Puebla, Chemistry of Materials, 2008, **20**, 1516.
33 X. Bai, X. Li and L. Zheng, Langmuir, 2010, **26**, 12209.
34 P. Ahonen, T. Laaksonen, A. Nykanen, J. Ruokolainen and K. Kontturi, Journal of Physical Chemistry B, 2006, **110**, 12954.

